Time-dependent spectral analysis of interactions within groups of walking pedestrians and vertical structural motion using wavelets

M. Bocian [a,*], J.M.W. Brownjohn [b], V. Racic [c], D. Hester [d], A. Quattrone [e], L. Gilbert [b], R. Beasley [b]

[a] Department of Engineering, University of Leicester, University Road, Leicester LE1 7RH, UK
[b] Vibration Engineering Section, University of Exeter, North Park Road, Exeter EX4 4QF, UK
[c] Department of Civil and Environmental Engineering, Politecnico de Milano, Piazza Leonardo da Vinci 32, Milano 20133, Italy
[d] School of Natural and Built Environment, Queen's University Belfast, Stranmillis Road, Belfast BT9 5AG, Northern Ireland, UK
[e] Department of Structural and Geotechnical Engineering, Politecnico di Torino, Corso Duca degli Abruzzi 24, Torino 10129, Italy

ARTICLE INFO

ABSTRACT

A multi-scale and multi-object interaction phenomena can arise when a group of walking pedestrians crosses a structure capable of exhibiting dynamic response. This is because each pedestrian is an autonomous dynamic system capable of displaying intricate behaviour affected by social, psychological, biomechanical and environmental factors, including adaptations to the structural motion. Despite a wealth of mathematical models attempting to describe and simulate coupled crowd-structure system, their applicability can generally be considered uncertain. This can be assigned to a number of assumptions made in their development and the scarcity or unavailability of data suitable for their validation, in particular those associated with pedestrian-pedestrian and pedestrian-structure interaction. To alleviate this problem, data on behaviour of individual pedestrians within groups of six walkers with different spatial arrangements are gathered simultaneously with data on dynamic structural response of a footbridge, from a series of measurements utilising wireless motion monitors. Unlike in previous studies on coordination of pedestrian behaviour, the collected data can serve as a proxy for pedestrian vertical force, which is of critical importance from the point of view of structural stability. A bivariate analysis framework is proposed and applied to these data, encompassing wavelet transform, synchronisation measures based on Shannon entropy and circular statistics. A topological pedestrian map is contrived showing the strength and directionality of between-subjects interactions. It is found that the coordination in pedestrians' vertical force depends on the spatial collocation within a group, but it is generally weak. The relationship between the bridge and pedestrian behaviour is also analysed, revealing stronger propensity for pedestrians to coordinate their force with the structural motion rather than with each other.

© 2017 The Authors. Published by Elsevier Ltd. This is an open access article under the CC BY license (http://creativecommons.org/licenses/by/4.0/).

1. Introduction

It is widely recognised that crowd dynamics are determined by local interactions between pedestrians and pedestrians and the environment [1]. For example, adaptations in gait patterns associated with collision avoidance can involve

* Corresponding author.
   E-mail address: m.bocian@leicester.ac.uk (M. Bocian).

intermittent changes in pacing rate, step length and walking velocity. Such behaviour can introduce non-stationary power at different frequency components in the spectra of the signals associated with pedestrian structural loading. Similar effects can occur due to psychological and sociological factors influencing behaviour of walkers. However, the nature of these gait adaptations in the context of structural stability is currently not well understood. As a consequence, a common practice in the development of crowd loading models on structures is to adopt an ansatz relating crowd density and the level of synchronisation of pedestrians' footsteps, or model pedestrian loading within a highly stochastic framework disregarding any deterministic relationships which can govern pedestrian behaviour.

The tendency for widespread synchronisation of pedestrians' walking frequencies and phases, hereafter referred to in a more general term as human-human interaction and abbreviated by HHI, has been one of the most often purported mechanisms affecting the stability of structural modes. The other mechanism is pedestrian-structure interaction, hereafter referred to in a more general term as human-structure interaction and abbreviated by HSI. This mechanism, pertaining to the energy feedback between pedestrian and structural motion, has been given more attention in recent years and indeed a considerable body of work already exists dealing with this problem; see e.g. [2–4] which cover this topic well. It is now generally accepted that walking pedestrians, on average, add damping and mass to the vertical vibration modes. Some uncertainties, however, still remain. While some sources report occurrences of synchronisation of pedestrian footsteps to the vertical ground motion [5,6], other suggest this propensity to be weak [7]. Furthermore, it is not known whether the HHI or HSI is the prevalent mechanism in the case of crowd loading.

Very few dedicated studies have so far been conducted to assess interpersonal gait coordination in the context of walking on flexible structures. Araújo et al. [8] used video recordings to determine the level of synchronisation among pedestrians walking in groups of different densities across 12 m long simply-supported slab, based on lateral motion of pedestrians' heads. No evidence of synchronisation between walkers was found in that study. Ricciardelli & Pansera [9] used pedometers to study gait characteristics and interactions of pedestrians in a crowd. A considerable variability in pedestrian behaviour was observed, pointing towards a need for further studies. To the best of the authors' knowledge, the only study reporting results from a flexible structure in situ, which mentioned the level of pedestrians' interpersonal synchronisation, is that reported in Van Nimmen et al. [10]. A set of wireless 3D motion sensors was used to record body motion of walkers crossing a footbridge. A step model of Li et al. [11] was fitted to these data to determine synchronisation of footsteps, although the rate of synchronisation was not quantified *per se* in that study.

More studies on interpersonal synchronisation in walking have been conducted in the fields of cognitive psychology, physical therapy and, broadly understood, human movement. It has been shown that visual information alone is generally a relatively weak stimulus for gait synchronisation [12,13]. However, tactile coupling, e.g. achieved by holding hands [14] or being connected at the waist level by an elastic link [15], significantly improved interpersonal synchronisation. Since these studies focused exclusively on a pair of test subjects walking either side-by-side or front-to-back, there is a need to expand the field of enquiry to account for more complex scenarios representative of walking in a crowd on real-life full-scale structures.

Considering the scarcity of data on pedestrian interactions while occupying structures capable of dynamic response and the uncertainty of the pedestrian loading and structural response models proposed in recent years, the purpose of this study is to propose a new framework for the assessment of interactions between the components of crowd-structure system. The proposed framework yields results suitable for the application in agent-based crowd models in which each pedestrian is modelled as a discrete particle. Since up to 70% of pedestrians in a crowd belong to a cohesive group [16], the behaviour of six pedestrians walking in groups of different spatial arrangements across a long-span footbridge is investigated together with the resulting structural response. The rest of the paper is organised as follows. Section 2 presents materials used and describes the conducted tests along with the methods applied in the analysis of the collected data. A new method of quantification of synchronisation between components of a system consisting of a structure and walking pedestrians is described in detail in Section 2.5. Although the proposed method is used in this study to analyse a vertical bridge motion due to the presence of a group of walking pedestrians, it is also applicable in the case of crowd loading on this and other types of structures exhibiting dynamic response in any direction. Section 3 presents the results of analysis conducted within the proposed method. Specifically, the strength and directionality of synchronisation between pedestrians is quantified in Section 3.1, while the strength of synchronisation between pedestrian and structural motion is quantified in Section 3.2. Concluding remarks are given in Section 4.

2. Materials and methods

This section gives details of the experimental tests conducted for the purpose of this study and methods of analysis of the collected data. Section 2.1 provides information on the structure chosen for the tests, Section 2.2 provides information on the participants, Section 2.3 provides information on the instrumentation deployed during the tests and Section 2.4 provides information on the applied experimental protocol. Section 2.5 presents a new method for quantification of interactions between components of a dynamical system consisting of a structure and walking pedestrians.

The experimental campaign was approved by the College of Engineering, Mathematics and physical Sciences Ethics of Research Committee at the University of Exeter.

2.1. The structure

Controlled tests with walking pedestrians were conducted on Baker Bridge (BB) in Exeter, UK. BB is an almost 109 m long cable-stayed footbridge located in vicinity of the Sandy Park Stadium serving as a home ground to the Exeter Chiefs rugby team. The bridge runs approximately North-South, such that its South end is closer to the stadium. Six pairs of cable stays attached at the top of 42 m high steel tower support a 3 m wide continuous deck sitting more than 10 m above the ground throughout most of its span. The tower is situated such that the lengths of the North and South spans supported by two and six pairs of stays, respectively, are in excess of 37 m and 71 m. An additional pair of cable stays anchors the tower to the North abutment. The deck is comprised of 49 tonnes of steel and 98 tonnes of concrete. The deck sits on a sliding pad bearing at the crossbeam of the tower, it is pinned at the North end, and has a sliding expansion joint at the South end. In elevation the deck falls 5.3 m from the North to the South end.

A modal testing campaign was performed on BB and its results are described in detail in [17–19]. To investigate the effect of pedestrian-structure interaction, this study focused on the response of BB in one vertical vibration mode, namely mode 3. The modal characteristics of BB for that mode are: 2 Hz for the frequency, 57.2 tonne for the modal mass and 0.32% for the damping ratio. The point of measurement of bridge response, which was approximately at the antinode, is shown in Fig. 1 together with the mode shape.

The bridge can be expected to be relatively lively due to the frequency of mode 3 falling into the range of typical pacing frequencies of walking pedestrians and also because the damping ratio of the mode is relatively low. Nevertheless, the bridge fulfils the stability requirements applicable at the time of its construction.

2.2. Participants

Six healthy subjects recruited from the cohort of undergraduate students at the University of Exeter participated in the experimental campaign. The basic data on all subjects, hereafter denoted as S1–S6, are given in Table 1. Each subject signed an informed consent form and completed physical activity readiness questionnaire prior to participating in experiments. The subjects wore their own casual clothes, suitable for the British weather conditions at the end of February (9 °C and 8 km/h wind on the testing day), and flat-sole shoes. The weather conditions during the modal testing campaign were similar, hence any aeroelastic effects which could in theory obstruct the assessment of HSI were highly unlikely to occur on these occasions. The subjects were informed that the purpose of the tests was to investigate the effects of walking pedestrians on the dynamic response of a footbridge and no other explanation was given in advance.

2.3. Instrumentation

A set of APDM Opal™ wireless motion monitors was used to obtain time-synchronised data on pedestrians' motion. Each subject was instrumented with a single monitor attached directly next to the skin with an elastic strap, at the level of fifth lumbar vertebra (L5). The vertical acceleration signals in world coordinate system, i.e. aligned with the gravity vector, were extracted from the captured data using quaternion algebra. It was shown in Bocian et al. [18] that signals resolved in this way, multiplied by pedestrian mass, give a reasonable approximation of the pedestrian vertical ground reaction force (GRF) both in terms of the amplitude and, more importantly in the context of this study, the timing. It was confirmed in the same study [18] that multiple monitors operating within a single wireless network remain synchronised when placed within the range of communication of their radio units which, depending on the environmental conditions, can stretch up to 30 m.

The response of BB was measured with an array of wired Honeywell QA quartz-flex low noise servo accelerometers as described elsewhere [17–19]. Having identified the dynamic properties of BB, a single point acceleration measurement
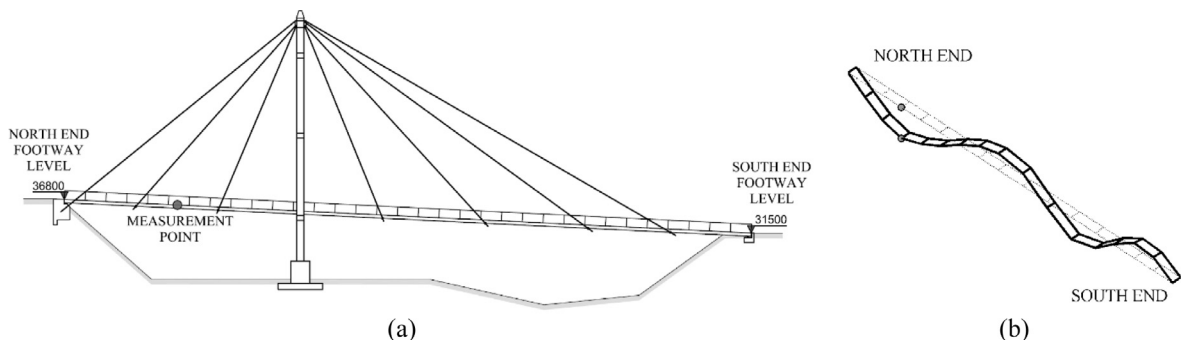

Fig. 1. (a) Elevation of the Baker Bridge. (b) The vertical mode shape considered, with frequency 2 Hz, modal mass 57.2 tonne and damping ratio of 0.32%. The point of measurement of BB response is denoted in (a) and (b) by grey dots.

Table 1
Basic data for all experimental subjects.

Subject	Gender	Mass [kg]	Height [m]
S1	Female	59	1.55
S2	Female	62	1.83
S3	Female	55	1.65
S4	Male	103	1.78
S5	Male	80	1.80
S6	Male	75	1.75

was used to determine BB behaviour in the considered vibration mode, as shown in Fig. 1, which is approximately at the antinode of the mode shape.

All captured data were sampled at 128 Hz.

2.4. Experimental protocol

The subjects participated in fifteen tests during which their walking formation was imposed as 3×2, 2×3 and 1×6 grids, where the first number denotes the number of columns aligned with the direction of progression, and the second number denotes the number of rows. These walking formations are hereafter referred to as $G_{3\times2}$, $G_{2\times3}$ and $G_{1\times6}$, respectively. The exemplar arrangements of subjects on BB are shown in Fig. 2.

Among the five tests performed with each walking formation, three tests were conducted at a normal speed and two at a slower speed representative of walking in a dense crowd. S1 always walked in the first row of any given grid and other subjects were instructed not to overtake S1. During all the tests at the slow speed the pacing rate of S1 was controlled by means of a metronome beat set to 1.6 Hz (= 96 bpm) and played on headphones. All other participants of the experiments were unaware of this feature of the experimental protocol. The pacing rate of S1 was not enforced in all tests at the normal speed to prevent any bias in the assessment of HSI in the considered vertical vibration mode at 2 Hz, which could occur by using the metronome set to coincide with that frequency. To minimise the effects of the repetitive spatial arrangement of pedestrians on the results, the position of S1 in the first row of the grid was randomised, except for $G_{1\times6}$, and so were the positions of all other subjects. A consequence of the adopted experimental protocol is that S1 did not participate in the interaction process to the same extent as other subjects did, but the behaviour of S1 was influential via setting the walking speed of the whole group.

The results of fourteen tests are reported in this study as a breach of experimental protocol occurred during one of the $G_{2\times3}$ tests conducted at the slower speed due to wrong metronome setting. Each test started and ended with subjects standing still at predefined positions just outside the boundaries of BB, according to the group arrangement prescribed for a given test, such that the distance covered by each subject and the duration of a test could be easily determined. The distances between pedestrians were not explicitly measured during the tests, but approximate values were obtained from the taken pictures. In the case of normal walking speeds, i.e. tests conducted without imposing the pacing rate on S1, the front-to-back and (where applicable) side-to-side distances between pedestrians measured between the midlines of their torsos were, respectively, approximately 1.4–2 and 0.8–1 m. For slower walking speeds, i.e. tests conducted while imposing the pacing rate on S1 by means of a metronome, the side-to-side distance between pedestrians remained the same (where applicable), but the front-to-back distance reduced to approximately 1.2–1.4 m.

The collected dataset is unique and valuable for the three main reasons:

- there have been no other studies known to the authors during which the pedestrians' force was determined on in-situ full scale structures simultaneously with the structural response, without having to extrapolate the amplitude and timing of that force;
- this is the most comprehensive dataset on pedestrians' stepping behaviour in real-life environment collected to date – it contains data from in excess of 13,000 steps from tests with different pedestrians' walking formations;
- there have been no adequate data recorded on crowd dynamics, pertinent to the problem of interpersonal synchronisation of footsteps to date.

2.5. Data processing

Of the very small number of reported studies on synchronisation of over-ground walking pedestrians, only a few have applied quantitative analyses. The so called *analytic signal* was constructed using Hilbert transform from the data collected from an accelerometer attached at the height of L5 of pairs of pedestrians walking side-by-side and used to establish an instantaneous phase of the walkers in Zivotofsky et al. [14]. Since the analytic signal is defined on the complex plane, it contains the instantaneous amplitude and phase information, the latter obtained from the inverse tangent of the quotient of the imaginary and real parts. However, the raw (i.e. unresolved) acceleration signal from L5 is not a good proxy of the vertical component of pedestrian's GRF [18] (hereafter denoted vGRF). Moreover, vGRF signal contains many harmonic components,

(a)

(b)

(c)

Fig. 2. Test subjects arranged in (a) $G_{3\times2}$, (b) $G_{2\times3}$ and (c) $G_{1\times6}$, walking on Baker Bridge.

including sub- and super-harmonics. Since an unequivocal definition of phase of such a multi-modal signal does not exist, the signal needs to be band-pass filtered. Therefore this method can lead to the misinterpretation and loss of information required to capture the true variability of pedestrian behaviour. To reduce uncertainty associated with filter settings and ambiguity in phase definition, a wavelet transform based approach to the determination of instantaneous pedestrian phase from walking gait data is proposed in this study.

The continuous wavelet transform $W_h(\tau, s)$ of the time series $h(t)$ relies on convolution of $h(t)$ with wavelet function $\psi_{\tau,s}(t)$ [20]:

$$W_h(\tau, s) = \int_{-\infty}^{+\infty} h(t)\psi_{\tau,s}^*(t)\mathrm{d}t \tag{1}$$

where τ accounts for the translation of wavelet in time t, s is the dilation parameter accounting for the varying wavelet scale, i.e. effectively stretching and compressing the wavelet, and * denotes complex conjugate applicable only for complex wavelet functions. In a general case, the wavelet function is often written as:

$$\psi_{\tau,s} = \frac{1}{\sqrt{s}}\psi\left(\frac{t-\tau}{s}\right) \tag{2}$$

where the term $1/\sqrt{s}$ is a weighting factor ensuring wavelets at different scales have the same energy [20]. An important task in any wavelet-based analysis is finding a suitable wavelet function ψ.

For the analysis of gait data from L5 resolved to vertical direction, i.e. aligned with the gravity vector, providing a proxy for vGRF, an appropriate wavelet function should effectively be a complex oscillatory filter. This is due to the near-periodic

nature of these data, reflecting the organisation of human gait and its adaptations to, broadly considered, environmental conditions. For its ability to capture the main features of the analysed signal, in particular its smoothly varying amplitude, complex Morlet wavelet was chosen herein as a wavelet function, given by [20]:

$$\psi(t) = \pi^{-1/4}\left(e^{i2\pi f_c t} - e^{-(2\pi f_c)^2/2}\right)e^{-t^2/2} \tag{3}$$

where $\pi^{-1/4}$ is the weighting factor introduced in Eq. (2) which can be omitted if phase information only is of interest, $i = \sqrt{-1}$ is the imaginary unit and f_c is the central frequency of the wavelet adopted in this study to be 0.955 Hz, corresponding to the angular frequency of 6 rad s^{-1}. The second term in the bracket in Eq. (3) is included to correct for the inadmissibility of Morlet wavelet, i.e. in that its mean is not zero for $f_c \approx 0$. The reason for the choice of f_c made herein is twofold. First, this choice introduces a symmetry in the Morlet wavelet in that for its real part the amplitude of the positive peaks immediately surrounding the central peak is approximately equal half the amplitude of the central peak, as can be seen in Fig. 3(b). Second, this choice renders the second term of Eq. (3) negligible hence the admissibility condition for the Morlet wavelet is satisfied by reducing Eq. (3) to:

$$\psi(t) = \pi^{-1/4}e^{i2\pi f_c t}e^{-t^2/2} \tag{4}$$

The first time-dependent term in Eq. (4) is a complex sinusoid allowing not just the amplitude but also the phase of the analysed signals to be established at different scales (or pseudo-frequencies, or pseudo-periods, since scale in wavelet analysis is not exactly equivalent to frequency or period), which is analogous to the Fourier transform, and the second term is a Gaussian window with standard deviation of unity.

The principle behind using a Morlet wavelet for analysing (total) vGRF is demonstrated in Fig. 3. The data in Fig. 3(a) were measured during a test with a male subject of mass = 75 kg and height = 1.8 m walking at a speed of 1.28 ms^{-1} with frequency of 1.75 Hz on a split-belt instrumented treadmill. The black and grey dashed curves in the figure show the vGRF applied by the right and left leg, respectively. It can be seen in Fig. 3(a) that vGRF for a step on each leg resembles a stretched letter 'M'. Force patterns from the same (right or left) leg are separated by periods of zero force during which the leg is off the ground and swinging.

It was shown in [18] that a single point inertial measurement from a suitable body landmark can be used as a proxy of (total) vGRF. Out of the four motion monitor placements tested in [18], i.e. the seventh cervical vertebra (C7; neck), sternum, navel and the fifth lumbar vertebra (L5), the best location for force reconstruction was found to be C7. This was not known at
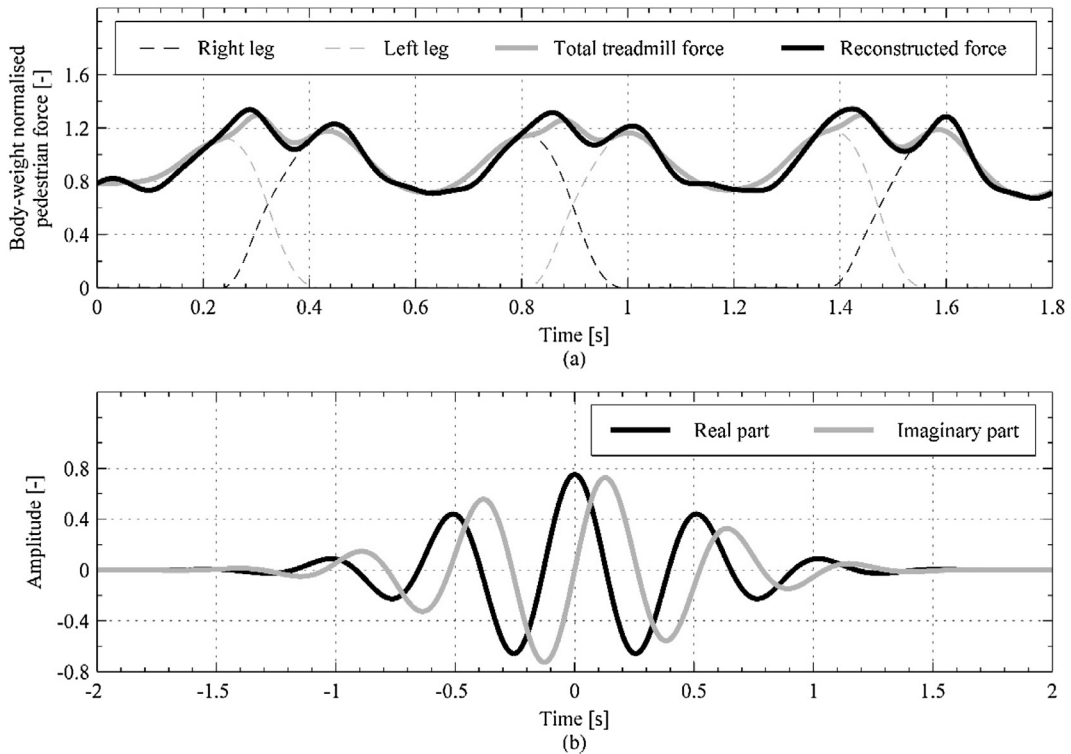

Fig. 3. (a) Exemplar truncated time history of pedestrian force measured on instrumented treadmill and reconstructed based on acceleration signal from L5 resolved to vertical direction, i.e. aligned with the gravity vector. (b) Exemplar real and imaginary part of the complex Morlet wavelet.

the time when the experimental campaign described herein was being planned hence a decision was made to instrument test subjects with monitors at the location of L5, which is known to be in proximity of the body centre of mass (CoM). Since the vertical acceleration signal from L5 (thick black curve) is representative of the motion of the CoM hence total vGRF, the corresponding signal from the treadmill is obtained by adding force traces from both legs (thick grey curve). It can be seen in Fig. 3(a) that the pattern of the total vGRF reconstructed based on data from L5 closely matches the total pedestrian force obtained from the instrumented treadmill hence these data can be used for the analysis of temporal pedestrian behaviour.

Fig. 3(b) presents examples of real (black curve) and imaginary (grey curve) parts of the complex Morlet wavelet used in the analysis of the collected data. Interestingly, it was found that over 95% of the wavelet power is typically contained within a single, relatively narrow band of scales across which the phase is fairly stationary at a given time, as shown in Section 2.5.1. Therefore analyses of temporal correlation of signals are focused on that band. This is equivalent to applying a narrow band filter using Hilbert transform approach, except that the phase obtained using wavelets is representative of the multi-modal characteristics of the analysed signal.

All numerical analyses were conducted in Matlab. For computational efficiency, wavelet transform was obtained with Fourier-based algorithm.

2.5.1. Synchronisation directionality based on bivariate phase difference distribution

The analyses of HHI and HSI were conducted using a bivariate approach, relying on pairwise (i.e. two at a time) consideration of correlation between signals. To this end, cross-wavelet transform between a pair of signals $\{x, y\}$ was calculated, defined as:

$$W_{x,y}(\tau, s) = W_x(\tau, s) W_y^*(\tau, s) \tag{5}$$

The phase difference was obtained directly from Eq. (5) as:

$$\phi_{x,y}(\tau, s) = \tan^{-1} \frac{\Im[W_{x,y}(\tau, s)]}{\Re[W_{x,y}(\tau, s)]} \tag{6}$$

where $\Im$ and $\Re$ denote imaginary and real part of the complex cross-wavelet transform coefficient $W_{x,y}(\tau, s)$. Since phase difference across scales of the largest cross-wavelet power at a given time is near stationary, a scalar time series of phase difference $\phi_{x,y}(t)$ is used to determine bivariate phase difference distribution. This was obtained by averaging phase difference at a given time over a range of these scales and is hereafter denoted as ϕ.

The relationship between the wavelet scale, s, and Fourier wavelength (or pseudo-period), λ_s, for Morlet wavelet is:

$$\lambda_s = \frac{4\pi s}{\omega_0 + \sqrt{2 + \omega_0^2}} \tag{7}$$

where $\omega_0 = 2\pi f_c$, and the pseudo-frequency is obtained from:

$$f_s = \frac{1}{s\lambda_s} \tag{8}$$

Therefore, for the chosen wavelet central frequency $f_c = 6$, the constant of proportionality between the scales and pseudo-period is 1.03.

As noted in Zivotofsky et al. [14], in quantifying phase difference based on vertical signals from L5 alone no distinction is made whether two walkers synchronised their step between ipsilateral legs, i.e. when both walkers are stepping on the same, e.g. right leg, at the same time, or between contralateral legs, i.e. when one walker is stepping on the right leg then the other is stepping on the left leg. This does not compromise analyses presented in this study where the focus is on vertical structural response since in this case, from the point of view of stability, both modes of synchronisation of pedestrian footsteps will have the same effect. This holds true when there is no coupling of modes, e.g. due to parametric resonance, which indeed is the case for BB. The convention of the phase difference is shown in Fig. 4. In order to facilitate the reading of the subsequent results, colour coding and arrows of different orientation are denoted therein to signify different phase difference ranges.

According to the adopted convention, for both modes of synchronisation described above (i.e. with ipsilateral and contralateral legs), the phase difference would be expected to consistently take a value of zero. Test subject S_m is leading and lagging subject S_n when ϕ takes values between $(0; \pi)$ and $(-\pi; 0)$, respectively. For the reader to better understand the subsequent analyses, in particular the significance of various phase difference patterns and their relationship with gait cycle events, exemplar data for two pairs of subjects are presented in Figs. 5 and 6.

Fig. 5(a) shows truncated time histories (between 29 and 37 s) of vertical L5 acceleration for two pedestrians S_m and S_n walking with different frequencies. In the figure it can be seen that S_m is walking with a slightly lower frequency than S_n meaning their steps are drifting in and out of phase. For example, at 33 s their steps are in phase whereas at 35 s they are almost exactly out of phase. Fig. 5(b) shows the magnitude of the cross wavelet transform of the full time series from 0 to 85 s. It can be seen that the large values exist in a narrow band of periods (or wavelet scales). This indeed confirms that, for walking data, this method overcomes the uncertainty with frequency choice associated with analytic signal concept [21]. The real part of the cross wavelet transform is plotted in Fig. 5(c) showing evolution of blue and red patches corresponding to
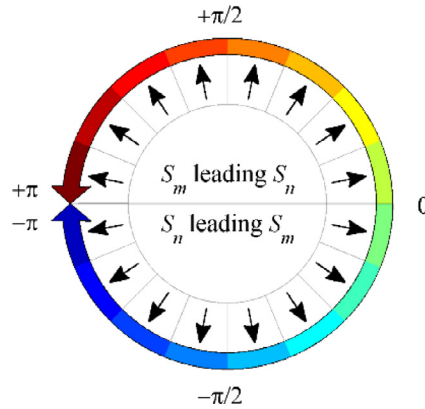
Fig. 4. The adopted convention for the phase difference between S_m and S_n.

periods of high and low correlation of pedestrians' motion, e.g. at 33 s and 35 s, respectively. The relative phase difference calculated with Eq. (6) is plotted in Fig. 5(d) where the direction of arrows indicates the localised phase difference (see Fig. 4). It can be seen that the phase difference is consistently non-stationary throughout the record and evolves approximately monotonically according to the beating frequency, i.e. the difference between the walking frequencies of S_m and S_n. In this case, given the record is sufficiently long, the phase difference is uniformly distributed throughout the whole range. However, for two pedestrians showing high degree of motion correlation this relationship does not hold. An example of this behaviour is shown in Fig. 6.

Fig. 6 shows the results of analysing data from subjects with similar walking frequencies. Fig. 6(a) shows the vertical L5 acceleration between 39 and 43 s when there is high in-step motion correlation and Fig. 6(b) shows period between 50 and 54 s when the step transitions are misaligned (see the double support periods in Fig. 3, when right and leg force signals are simultaneously present), respectively. The phase difference is fairly stationary throughout the record, which can be deducted from Fig. 6(d) showing the real part of cross wavelet transform. For completeness, the magnitude of that transform is shown in Fig. 6(c). Although some leakage of energy to lower periods can be visible (below 0.1 s), the great majority is again confined to a small band of periods (or wavelet scales). Clearly, there is a strong bias in the distribution of phase angles in Fig. 6 (e) towards values around $-\pi/4$ which means that, according to the adopted convention (see Fig. 4), S_n was leading S_m for a major part of the test.

It needs to be pointed out that the leader-follower casualty is arbitrary. This is because bivariate phase analysis includes a known intrinsic mathematical ambiguity associated with equivalency in phase angle definition. This is to say that for two signals shifted by a known phase, the lead-lag relationship depends on the point of reference.

The distortion of patches at the borders of the window is caused by the edge effects, i.e. the values of the transform close to the boundaries of the signal being computed incorrectly due to zero padding. In order to highlight the region in which this uncertinty applies a cone of influence is shown in Fig. 5(b)–(d) and Fig. 6(c)–(e) in white. Since the subjects were stationary at the beginning and end of the shown records, meaningful phase difference information comes from the regions of the plots corresponding to the region of occurrence of arrows in Fig. 5(d) and Fig. 6(e).

2.5.2. Synchronisation strength based on Shannon entropy

Synchronisation strength in HHI and HSI was calculated using an approach based on Shannon entropy of bivariate phase difference distribution, defined as proposed in [22]:

$$E = -\sum_{k=1}^{N} p_k \ln p_k \tag{9}$$

where p_k is the probability of $\phi_{x,y}(t)$ falling into bin k and N is the number of bins, here having size $\pi/8$. For the results to be comparable between different tests, they were normalised by maximum Shannon entropy representative of the case of perfect frequency synchronisation $E_{\max} = \ln N$, yielding synchronisation strength index:

$$\gamma = \frac{E_{\max} - E}{E_{\max}} \tag{10}$$

According to this convention, $\gamma = 0$ implies perfectly uniform distribution of ϕ while $\gamma = 1$ implies perfect frequency synchronisation, i.e. constant ϕ, during a given test. In the implementation of this method for experimental data the latter result is practically impossible to obtain due to the presence of noise in the measured signals [21]. The directionality of synchro-
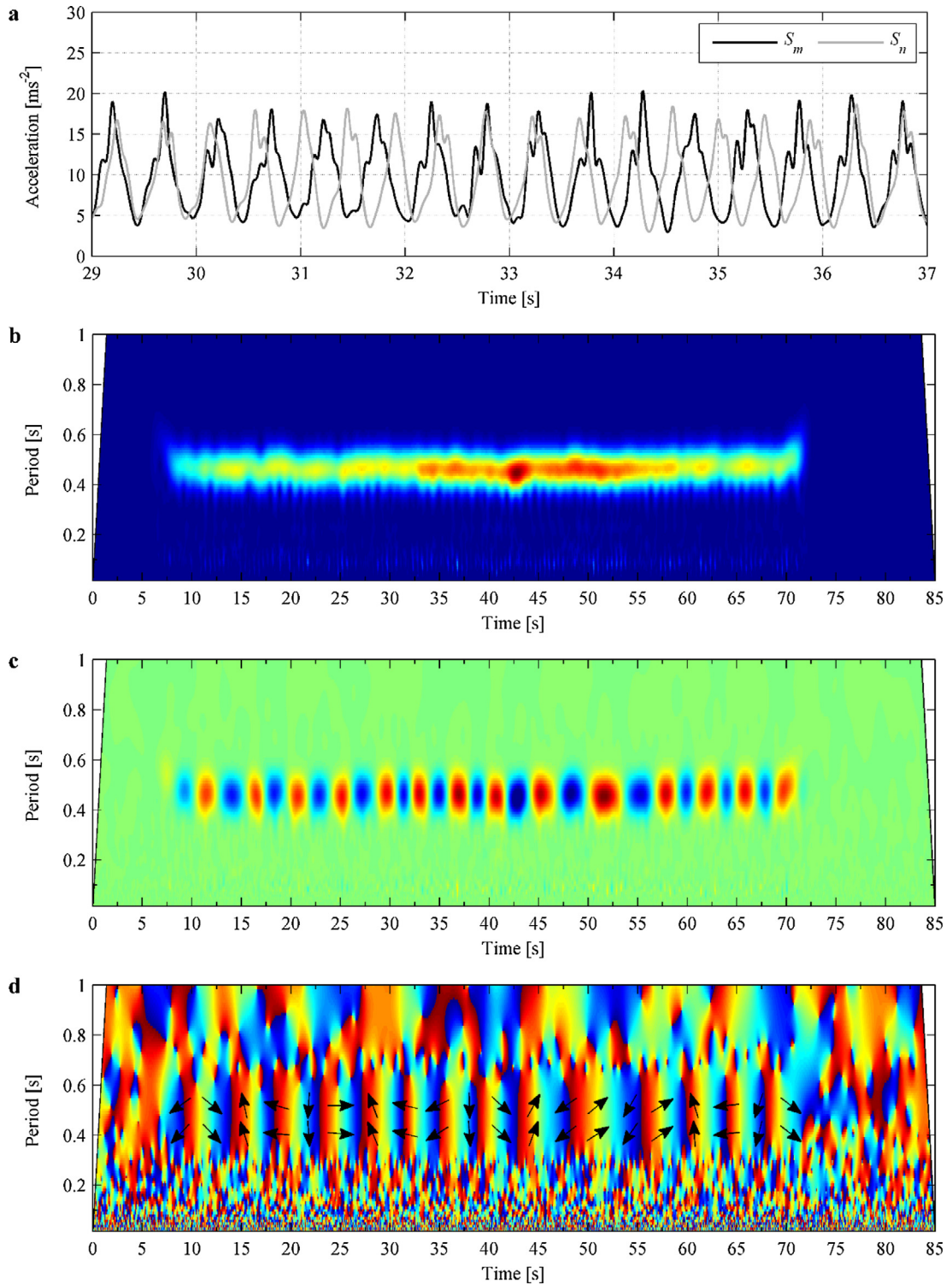
Fig. 5. (a) Truncated time histories of vertical L5 acceleration from two subjects walking with different frequencies. (b) Magnitude of cross wavelet transform. (c) Real part of the cross-wavelet transform. (d) Phase difference based on the cross-wavelet transform with arrows indicating localised phase difference in the area of concentration of the largest power. All data in the figure come from the same test. The cone of influence is shown in white in (b), (c) and (d).
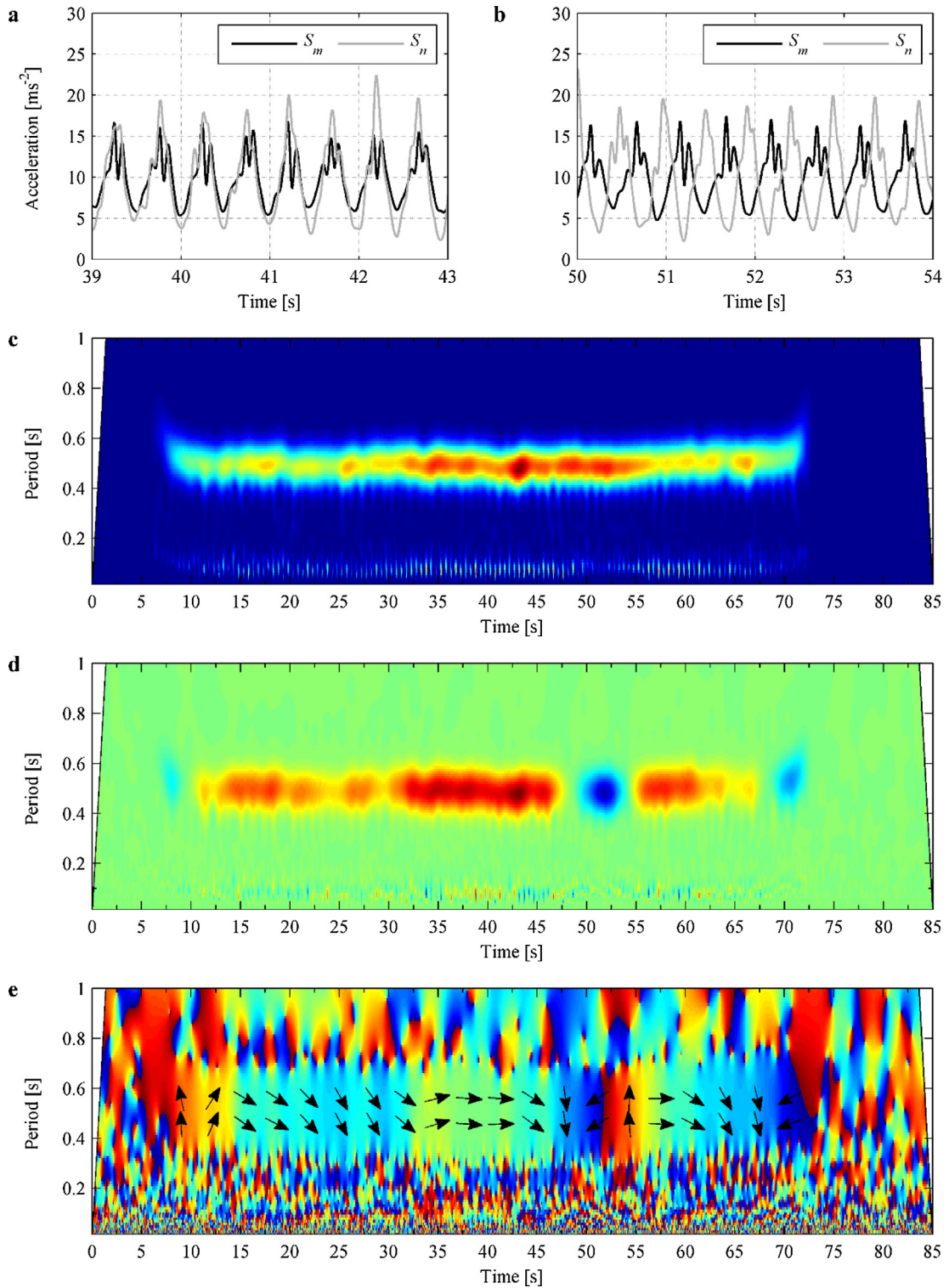
Fig. 6. Truncated time histories of vertical L5 acceleration from two subjects showing walking in-phase (a) and out-of-phase (b). (c) Magnitude of cross wavelet transform. (d) Real part of the complex cross-wavelet transform. (e) Phase difference based on the cross-wavelet transform with arrows indicating localised phase difference in the area of concentration of the largest power. All data in the figure are from the same test. The cone of influence is shown in white in (c), (d) and (e).
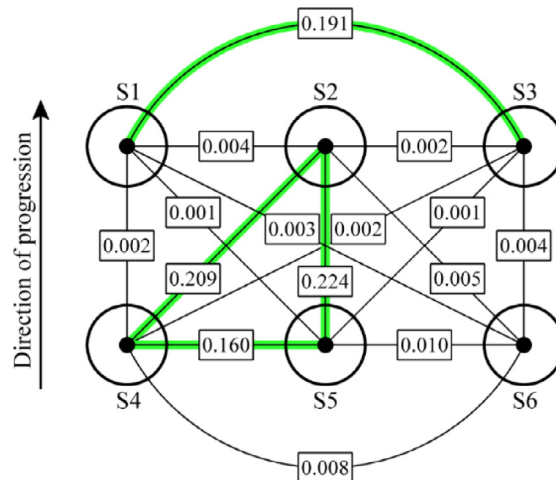
Fig. 7. Subject-oriented map of pedestrian-pedestrian interaction strength based on data from a single test.

nisation is also worth considering as it could cause pedestrian loading to have a different influence on structural response, e.g. effectively damping or putting energy into the vibrating mode. Given ϕ is described on an angular scale, the methods of circular statistics were applied in quantitative analyses of directionality in Section 3.1.4.

An exemplar subject-oriented map of interactions between six pedestrians crossing BB in $G_{3\times2}$ is shown in Fig. 7. The test subjects (see Table 1) were located such that S1, S2 and S3 were at the top row and S4, S5 and S6 were located at the bottom row, and walked at a normal speed, i.e. without imposing metronome beat (see Section 2.4). The values in boxes are the synchronisation indices between each pair of subjects obtained from Eq. (10). Relatively strong correlation of pedestrians' vGRF is visible for the four highlighted connections.

To facilitate understanding of data in Fig. 7, corresponding histograms of phase difference are shown in Fig. 8. In the calculation of these histograms the first signal was taken from the subject denoted on the vertical axis and the second signal from the subject denoted on the horizontal axis (see Eq. (5)). Therefore, according to the adopted convention (see Fig. 4), S3 was leading S1, S4 was leading S2 and S5 was leading S2 for the majority of the test duration since the histogram data for these pairs of subjects are more densely populated in the positive range of values. As could be expected from the definition of the synchronisation strength index in Eq. (10), the histograms of phase difference data for all connections bearing small values in Fig. 7 resemble a uniform distribution.

A subject-oriented map, such as the one in Fig. 7, can be used to uncover the strength of interaction between each pair of subjects during a given test. However, a better understanding of relationships between pedestrians can be obtained by looking at the results in the light of causal inference, i.e. the relationship between the stimulus and the effect. Therefore, rather than focusing on synchronisation strength between specific subjects, in most of the subsequent analysis of HHI, the attention is given to their relative location within the walking formation.

3. Results and discussion

3.1. Pedestrian-pedestrian interaction

Multi-agent crowd models in which each pedestrian is represented by a particle subjected to physical and social forces require an input in the form of laws governing pedestrian behaviour. Although synchronisation is sometimes accounted for in these models [23–27], the strength of this effect and its directionality is always assumed arbitrarily. In order to allow these models to be advanced, data on real pedestrian behaviour is required, presented in a form allowing a coupling force to be defined. In the context of the pedestrian-pedestrian interaction, an interaction map in which the strength and directionality of synchronisation is assigned to the position of a pedestrian relative to fellow pedestrians within the walking formation provides means of meeting this requirement. Therefore a map of synchronisation strength obtained with Eq. (10) is first presented in Section 3.1.1, hereafter referred to as a topological map of pedestrian interactions. The choice of this terminology was dictated by the analogy with the term *topology* in mathematics, used to refer to the properties of space, the term *network topology* in communication, used to refer to the arrangement of various network components and their relations, and the term *topological map* in cartography, used to refer to a type of simplified diagram showing relationships between different points. The influence of walking formation, height difference between a pair of pedestrians and their gender on synchronisation strength are then analysed in Sections 3.1.2 and 3.1.3. The directionality of synchronisation is quantified by means of circular statistics based on phase difference distribution in Section 3.1.4.
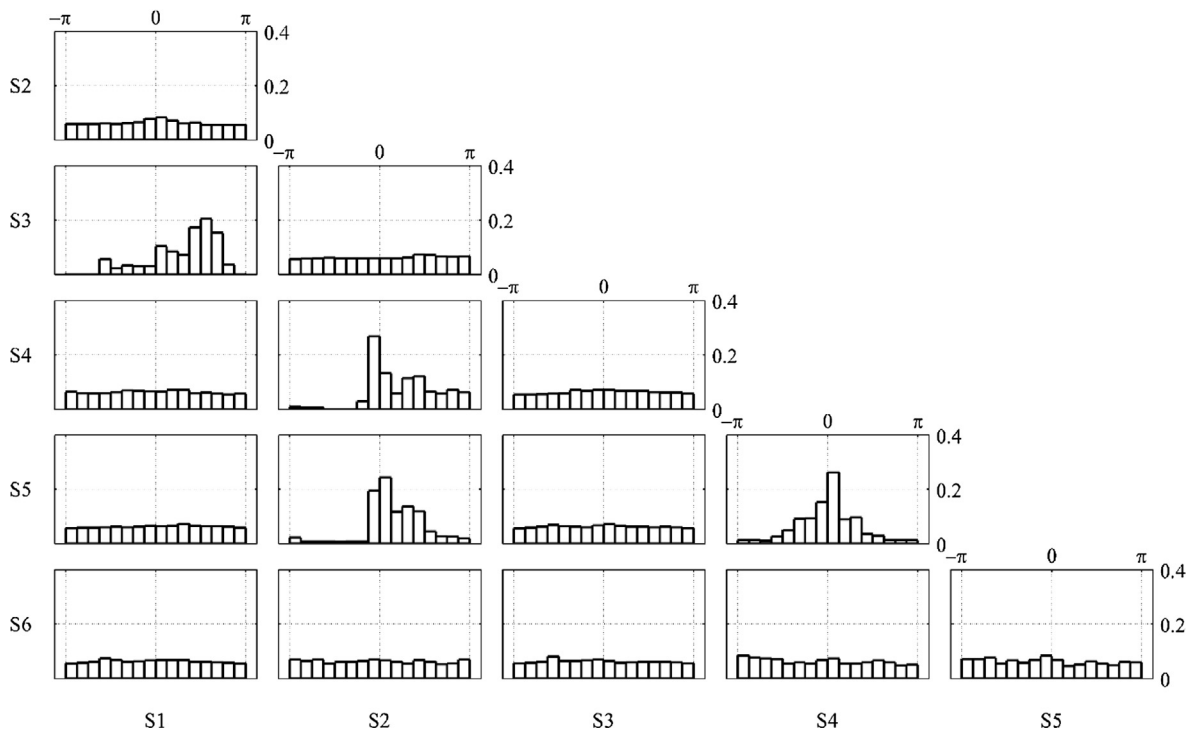
Fig. 8. Unity-normalised distributions of phase difference for all pairs of subjects during the test from which results are presented in Fig. 7.

3.1.1. Topological map of pedestrian interactions

It can be hypothesised that visual perception provides a stimulus for coordination of gait between walkers. Therefore, all the results pertaining to each pedestrian formation were decomposed into interaction-oriented map. Such a map is a representation of the strength of interaction according to the location of stimulus source relative to an observer, disregarding their identity. Importantly, the term *observer* is used here in relation to the capacity for visual perception, without discounting the role of an observer as a participant of the process leading to a state of their gait being in some degree of synchrony with the gait of another pedestrian. The field of view of human binocular vision, i.e. the extent of the visual world perceptible by an observer, spans approximately 200° horizontally and 135° vertically [28]. Accordingly, it is reasonable to limit the scope of the interaction-oriented map to locations within the semicircle in front of the observer, assumed split in half by the axis aligned with the direction of progression which, in the circumstances of the conducted tests, might be assumed parallel to the longitudinal axis of the bridge.

Interaction-oriented maps for all three pedestrian formations are presented in Fig. 9. The synchronisation strength index was obtained by averaging synchronisation strength indices between results for all pairs of subjects and all tests in which a considered subjects' collocation occurred. For example, side-by-side (i.e. shoulder-to-shoulder) walking occurred in all tests in $G_{3\times2}$ and $G_{2\times3}$, but not in $G_{1\times6}$. Since there were five tests conducted with each walking formation, but the results from one test in $G_{2\times3}$ cannot be considered (see Section 2.4), the results from nine tests were used to obtain the synchronisation strength index for side-by-side walking. Furthermore, since four and three pairs of subjects walked side-by-side during each test in $G_{3\times2}$ and $G_{2\times3}$, respectively, there were thirty-two occurrences of this collocation. For all pairs of subjects located side-by-side, even when separated by another subject, the synchronisation strength was calculated from all tests in which a given connection occurred for a given walking formation. Since in this case both subjects can act as an observer and stimulus source (as they remain within each other's field of view), the values of synchronisation strengths between the corresponding collocations to the right and left of an observer are the same. This is not the case for all diagonal subjects' arrangements since, in bivariate analysis framework, only one subject can then act as an observer and the other can only act as a stimulus source.

The highest synchronisation strength in Fig. 9(a) (at 0.031) appears for stimulus generated by a pedestrian located diagonally to the right from the observer, but it is very close to the synchronisation strength between the observer and stimulus located directly side-by-side (at 0.030). The highest synchronisation strength in Fig. 9(b) is found for stimuli generated by pedestrians located directly in front of an observer (at 0.065) or to the side (at 0.050). The highest synchronisation strength in Fig. 9(c) is found for stimulus generated by a pedestrian directly in front of an observer (at 0.071). Therefore, overall, the results presented in Fig. 9 seem to confirm what could be expected, i.e. the strongest stimuli for synchronisation generated by pedestrians in the closest vicinity to an observer.
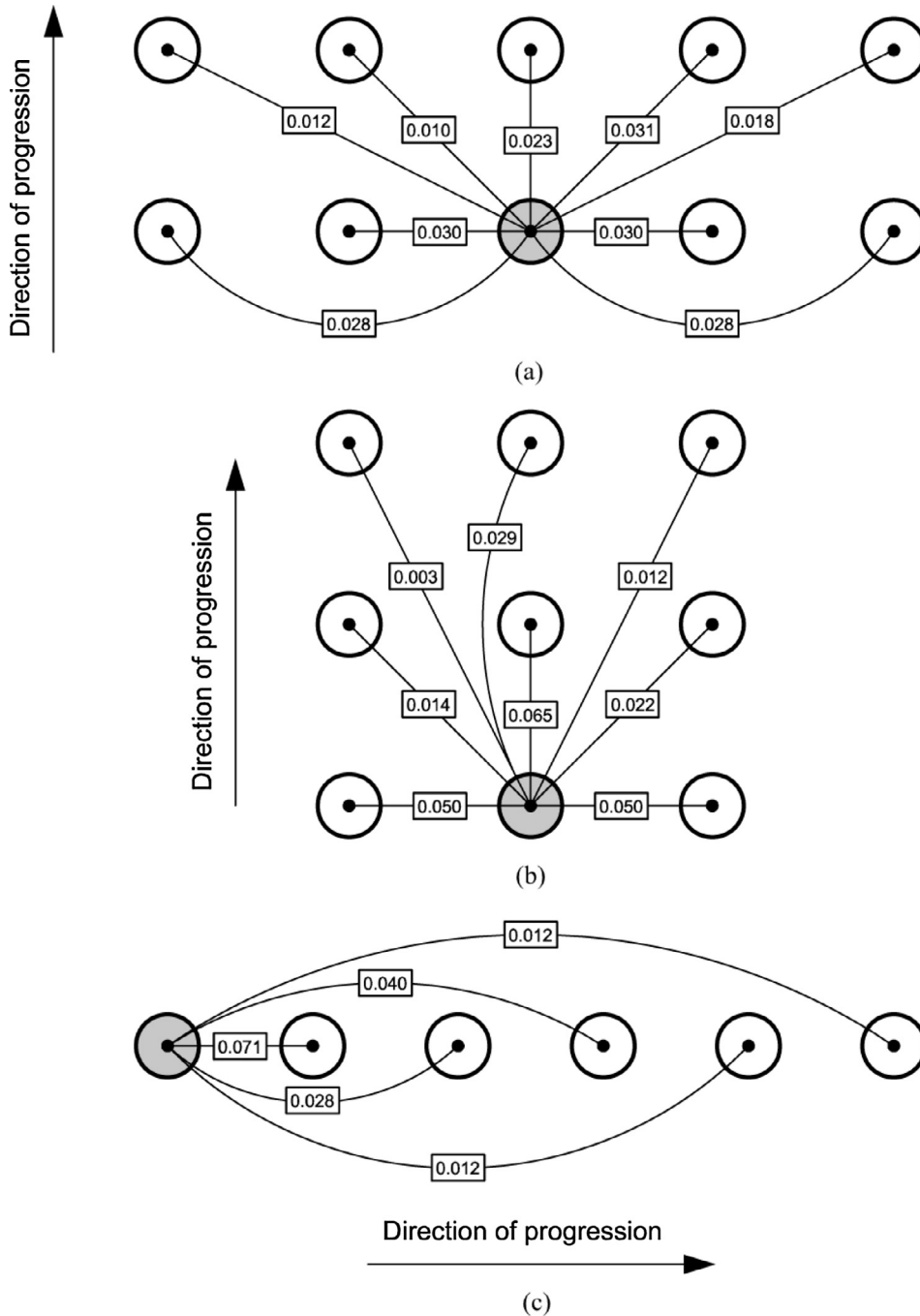
Fig. 9. Topological maps of pedestrian-to-pedestrian interaction strength for walking formations: (a) $G_{3\times2}$, (b) $G_{2\times3}$ and (c) $G_{1\times6}$.

It is noteworthy that the strength of interactions in Fig. 9(a) and (b) varies between the corresponding diagonal locations of stimulus source in the right and left directions (relative to the direction of progression). There seems to be a persistent effect in that synchronisation strength for locations to the right of an observer is consistently higher than for those to the left. It can be hypothesised that the observed stronger tendency to synchronise with pedestrians to the right of the observer is associated with ocular dominance.

Ocular dominance refers to a tendency to prefer information perceived by one eye to information perceived by the other [29]. It is estimated that in the case of sighting, i.e. for tasks testing eye rivalry requiring eyes to be pointed straight ahead, on average approximately 70% of population shows preference for the right eye [29]. Although what role this laterality of eye functioning plays in visual or oculomotor processes is not yet fully understood [30], some more recent research on the topic

has shown that ocular dominance plays an important role in binocular tasks such as feature search [31], i.e. detection of a target element from an assembly of other elements differing from the target element in one visual feature only, and conjuncture search [32], i.e. detection of a target element from an assembly of other elements having common and different features to those of the target element. In the view of Shneor & Hochstein [31,32], it can be expected that "inputs from the dominant eye may be more sensitive, responsive or numerous, and/or may capture attention more readily, leading to a more salient percept".

In order to test this postulate, the Hutcheson *t*-test [33] was carried out on data from the histograms obtained from cumulative phase difference distribution from the corresponding diagonal collocation between the observer and synchronisation stimulus in the right and left directions for a given walking formation. A significance level of 5% ($p = .05$) was adopted meaning that the null hypothesis, stating that the synchronisation strengths of both samples are the same, is rejected if their probability of being the same is less than 5%. Statistically significant difference was found for all considered connections. Although statistical analysis seems to support the notion of the influence of ocular dominance, since the conducted tests were not specifically designed to address this issue, further research is currently underway to gain confidence in this effect.

The information presented in Fig. 9 is combined in Fig. 10 to produce an interaction-oriented map of pedestrian-pedestrian interaction strength based on data from all tests. In derivation of synchronisation indices in Fig. 10 all values from corresponding visual stimuli locations for different formations were averaged using weighted arithmetic mean, i.e. taking into account the number of occurrences of a given connection. Furthermore, the results from corresponding locations to the right and left of an observer were taken as equivalent. It can be seen in Fig. 10 that the highest synchronisation index, 0.056, occurs between an observer and the pedestrian directly in front of them. The next highest synchronisation index, 0.04, is found for a pedestrian in front of and separated with an observer by two other pedestrians. This is a rather surprising result, which might be caused by the effect of walking formation, discussed in Section 3.1.2. The next highest synchronisation index, 0.038, is found for a pedestrian directly to the side of an observer. Interestingly, the synchronisation indices for pedestrians directly in front and to the side of an observer, but separated by one other pedestrian, are also relatively high, at 0.028. This may indicate network permeability (or connectivity), i.e. transfer of information (here synchronisation stimulus) between pedestrians. The synchronisation index for a pedestrian located directly to the side and in front of an observer is 0.02, while the synchronisation indices for all remaining pedestrian locations with whom a visual link is either obstructed or distant fall at or below 0.015.

Clearly a pedestrian walking in a group is most likely to synchronise their steps with a pedestrian directly in front or to the side. A dilution (or cascading) of information (or stimulus leading to a state characterised by some degree of synchronisation) occurs the farther the stimulus source is located from an observer. In other words, the synchronisation field strength diminishes with the distance and interference.

Although the synchronisation strength is overall rather low, the influence of the discussed effects on crowd and bridge dynamics cannot be easily discounted. This is because it is the weak interactions between pedestrians which can drive emergent crowd behaviours. Furthermore, the interaction between a pair of pedestrians during a given test can yield a much higher synchronisation index than the average values presented in Figs. 9 and 10. This is exemplified by the results presented in Figs. 7 and 8 where the highest synchronisation index is 0.224 for a pair of pedestrians walking front-to-back. This issue will be further discussed when analysing phase difference distribution in Section 3.1.4.

3.1.2. The effect of walking formation

In the previous section the strength of synchronisation was assigned to a pedestrian topological map. However, it is also useful to know if different pedestrian formations can be expected to yield different synchronisation strengths. This is because bridges of different widths or pathway arrangements may promote different pedestrian formations which, if the hypothesised effect were true, can in turn influence the amplitudes of pedestrian loading and structural response. To address this postulate, the average synchronisation strength was calculated for tests conducted with pedestrians walking in different formations using weighted arithmetic mean. The following results were obtained: 0.024 for formation $G_{3\times2}$, 0.037 for formation $G_{2\times3}$ and 0.042 for formation $G_{1\times6}$. Clearly, the more linkages in the grid in which the pedestrians are faced front-to-back, the stronger the average synchronisation index. This is consistent with the results presented in Section 3.1.1.

It should to be noted that the bridge width is not the only determinant of walking formation. Self-organisation phenomena in a crowd can also lead to the formation of lanes in which pedestrians are moving uniformly in the same direction, which is associated with minimising the energy spent on collision avoidance manoeuvres [34].

3.1.3. Height and gender effects

It is well known that the pedestrian height, walking velocity and stride frequency have a strong correlation [35]. Therefore, since the walking speed was imposed in experiments by a requirement of preserving grid position (hence spatial group cohesion), a stronger tendency to synchronise could be expected for subjects of similar height (see Table 1). In order to assess this postulate, an average synchronisation index based on Shannon entropy was calculated from all conducted tests for each pair of subjects. The results are presented in Table 2.

It can be seen in Table 2 that the highest average synchronisation index (0.093) was obtained for a pair S1 and S3, in which both subjects were females of height 1.55 m and 1.65 m, respectively. Interestingly, they were also two of the shortest subjects within the whole group. To investigate this further, the information on pedestrian-to-pedestrian synchronisation strength, corresponding height difference and gender is combined in Fig. 11.
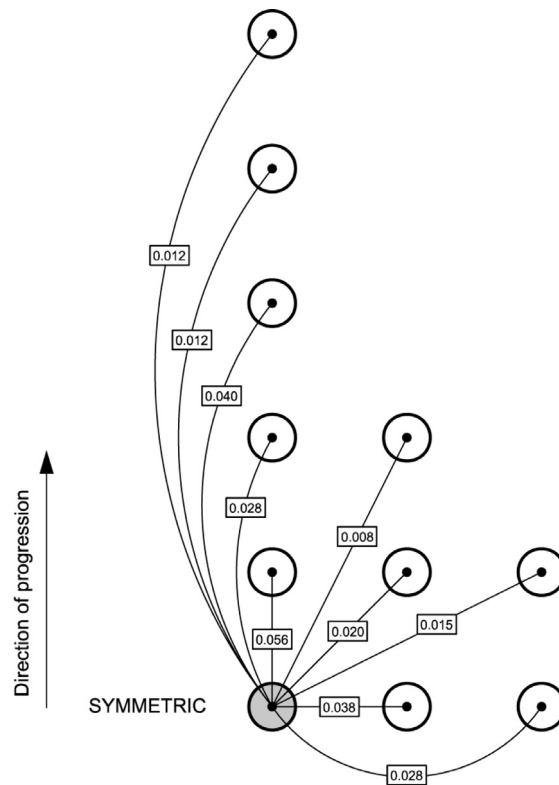
Fig. 10. Topological map of pedestrian-to-pedestrian interaction strength based on data from all tests.

Table 2
The average synchronisation index derived based on Shannon entropy for each pair of subjects over all tests.

	S1	S2	S3	S4	S5
S6	0.025	0.017	0.003	0.065	0.042
S5	0.016	0.082	0.009	0.063	
S4	0.019	0.052	0.004		
S3	0.093	0.013			
S2	0.004				

Clearly, the results for gender-homogenous pairs are scattered on the plot hence inconclusive. However, it is evident that the subjects are more likely to synchronise their steps if they are of similar height. This agrees with observations in [36]. A phenomenological explanation of this effect is offered here on the basis of optimisation of gait. In short, optimisation of gait relies on adaptation of locomotor patterns in order to fulfil a cost function [37]. In the absence of other objectives (e.g. stability or speed requirements), the most important cost function is the expenditure of energy – a staple commodity for all living organisms [38]. For two pedestrians of similar height, their preferred and optimal (from the point of view of energy efficiency) walking frequencies for a given walking speed are most likely to also be similar [39]. Visual cues from movement of a fellow pedestrian walking in the closest vicinity (i.e. positioned directly in front, shoulder-to-shoulder or diagonally in front) provide a stimulus for gait rhythmicity. Relatively small adjustments in locomotor patterns, if any, are required to establish (consciously or not) a common gait rhythm, without incurring much energy expenditure. However, if the pedestrians' heights differ considerably, the energy optimisation requirement overcomes the tendency to synchronise and the pair of pedestrians is less likely to entrain their steps. The above argument assumes a synchronised state, but without pointing towards any particular phase difference, is an attractrix (i.e. a relatively wide set of locus of attraction) of the (dynamical) system consisting of two pedestrians walking in close proximity, when visual motion cues are available. This is supported by findings in [15].

3.1.4. Phase difference distribution

The analyses presented so far focused on the topological strength of interaction between pedestrians. However, an insight into casualty of these interactions can also be gained by examining the phase difference distribution. Therefore the phase difference data were analysed using a method of circular statistics [40]. The results in terms of mean circular direction, $\bar{\phi}$,
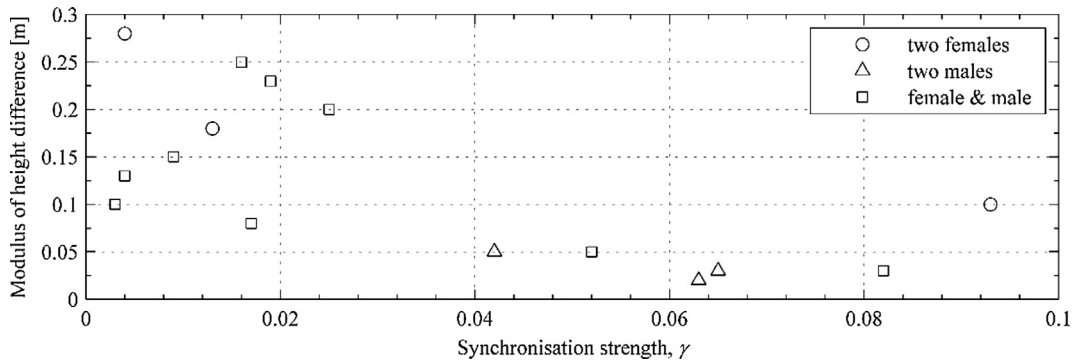
Fig. 11. The relationship between the strength of synchronisation derived based on Shannon entropy, averaged over all tests for each pair of subjects, and the difference in subjects' height. Gender information is included on the plot by different markers.

Table 3
Statistical measures of directionality of phase difference distribution.

Connection	Number of occurrences	Speed N = normal S = slow	Sync strength index γ	Mean circular direction [rad] $\bar{\phi}$	Mean resultant vector length R	Circular deviation σ	Kurtosis k	Skewness b
$C_{1,0}$	21	N	0.0036	−0.0087	0.0887	1.3501	0.0279	0.0108
$C_{1,0}$	11	S	0.0023	0.7588	0.0427	1.3837	−0.0438	−0.0230
$C_{2,0}$	6	N	0.0089	−1.4443	0.1003	1.3414	0.0668	−0.0505
$C_{2,0}$	4	S	0.0011	−1.1722	0.0333	1.3905	−0.0256	−0.0099
$C_{0,1}$	36	N	0.0038	0.5094	0.0787	1.3574	0.0298	−0.0294
$C_{0,1}$	20	S	0.0137	0.9151	0.1927	1.2706	0.0351	0.0195
$C_{0,2}$	18	N	0.0023	−2.3064	0.0623	1.3694	0.0053	−0.0214
$C_{0,2}$	10	S	0.0036	2.3471	0.0941	1.3460	0.0137	−0.0133
$C_{0,3}$	9	N	0.0057	−2.8934	0.1026	1.3397	0.0564	−0.0047
$C_{0,3}$	6	S	0.0027	−2.4684	0.0192	1.4006	−0.0386	0.0165
$C_{0,4}$	6	N	0.0015	0.4074	0.0275	1.3946	−0.0282	−0.0036
$C_{0,4}$	4	S	0.0036	−1.2459	0.0837	1.3537	0.0324	−0.0172
$C_{0,5}$	3	N	0.0017	−0.9266	0.0396	1.3859	0.0145	0.0058
$C_{0,5}$	2	S	0.0056	−0.9727	0.1041	1.3386	0.0267	−0.0342
$C_{1,1}$	24	N	0.0013	0.2307	0.0383	1.3869	0.0124	0.0076
$C_{1,1}$	12	S	0.0015	−0.0885	0.0475	1.3802	0.0059	0.0113
$C_{2,1}$	6	N	0.0036	0.7525	0.0738	1.3611	0.0038	0.0302
$C_{2,1}$	4	S	0.0019	1.2326	0.0275	1.3946	−0.0075	0.0525
$C_{1,2}$	6	N	0.0011	0.4629	0.0310	1.3921	0.0167	0.0188
$C_{1,2}$	2	S	0.0082	0.1543	0.1100	1.3342	−0.0764	−0.0023

For $C_{i,j}$ i = lateral separation, j = anterior separation. The phase difference was always calculated from the leftmost or rearmost subject towards the other subject for pairs of pedestrians walking in the same row or column, respectively. For all diagonal connections (when i ≠ 0 and j ≠ 0), phase difference was always quantified relative to the rearmost pedestrian.

mean resultant vector length, R, standard deviation, σ, kurtosis, k, and skewness, b, are presented in Table 3. In the calculation of R all phase difference values are first transformed to two-dimensional unit vectors: $r_i = (\cos \phi_i \quad \sin \phi_i)$ and then averaged over all data samples i, while $\bar{\phi}$ was obtained by using the four quadrant inverse tangent function on R [40].

Two sets of results are shown for each topological connection, $C_{i,j}$, differentiating between walking with freely chosen (by S1) and metronome-imposed pace. Subscripts i and j denote lateral, i.e. to the left and right relative to the walker, and anterior, i.e. to the front relative to the walker, separation between pedestrians in the walking grid, respectively. The phase difference was always calculated from the leftmost or rearmost subject towards the other subject for pairs of pedestrians walking in the same row or column, respectively. For all diagonal connections (when i ≠ 0 and j ≠ 0), phase difference was always quantified relative to the rearmost pedestrian. For example, according to this convention, $C_{1,1}$ indicates that the phase difference statistics are quantified for a pair of pedestrians located diagonally within the grid, such that one of them is in front and to the right or left relative to the other. All statistical measures in Table 3, including synchronisation strength indices, were obtained from a set of all phase difference values for a given topological connection. For example, a set of phase difference values for $C_{1,0}$ at normal walking speed contained data from 21 pairs of subjects, as denoted in the second column of Table 3. Admittedly, the data samples for the most distant pairs of subjects are relatively small, e.g. the results for $C_{0,5}$ are based on data from 2 pairs of subjects only. Consequently, these results should be taken with care.

It can be seen in Table 3 that $\bar{\phi}$ generally varies between normal and slow walking and takes a wide range of values. The closer R is to unity, the higher concentration of data points around the sample mean. The highest value of R is 0.1927 for $C_{0,1}$
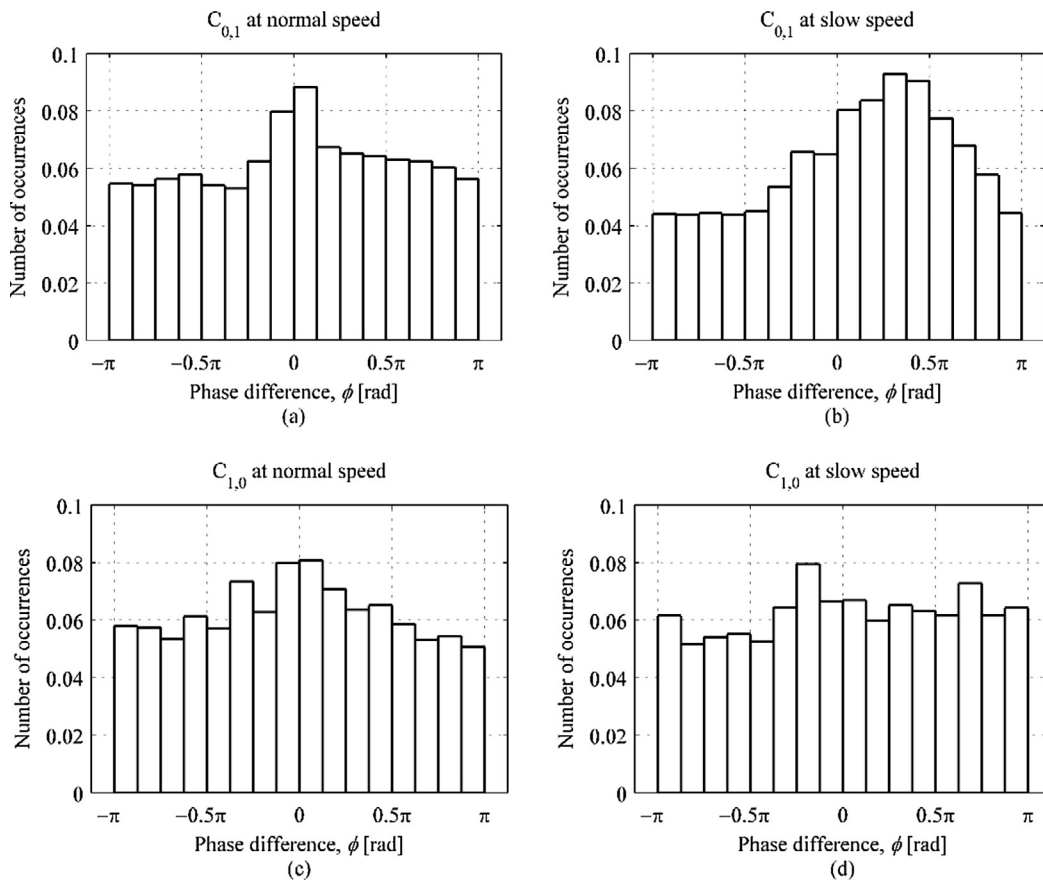
Fig. 12. Exemplar unity-normalised phase difference distributions for a pair of pedestrians walking front-to-back: (a) and (b), and side-by-side: (c) and (d), for normal and slow speed, respectively.

and slow walking. The distribution of ϕ was first tested for uniformity using Rayleigh test, adopting significance level of 0.05. In all cases, the null hypothesis stating the distribution is uniform was rejected. σ is described on interval from 0 to $\sqrt{2}$. Unsurprisingly, the lowest value of σ is for $C_{0,1}$ and slow walking. The closer the value of k is to unity, the stronger the peakedness of the distribution, and the closer the value of b is to zero, the more symmetric the distribution is around $\bar{\phi}$. In all cases the data are relatively little peaked and rather symmetric.

For the reader to better understand the relationships quantified in Table 3, exemplar phase difference distributions for $C_{0,1}$ (front-to-back walking) and $C_{1,0}$ (side-by-side walking) are presented in Fig. 12(a) & (b) and (c) & (d), respectively. It can be seen that in the case when the walking pace is freely chosen by S1, there is a slight tendency to walk in step for $C_{0,1}$ and $C_{1,0}$, bearing in mind no distinction is made in this study between steps initiated with ipsilateral and contralateral legs. In the case when the pacing frequency of S1 is prompted by a metronome set to 1.6 Hz hence for lower walking speeds, there is a clear tendency for $C_{0,1}$ for the follower to initiate steps faster than the leader. This might be associated with anticipatory strategy in adaptive stepping behaviour, whereby the follower will try to reach double-support phase of gait slightly faster than the leader. Since both legs are then in contact with the ground, the stance is more stable and corrections to the body motion can be implemented more easily in order to avoid collision with the leader or to preserve grid cohesion. No trend is seen in data in Fig. 12(d). Considering these data in the context of the results in Fig. 12(b), it is likely that controlling ones walking speed and collision avoidance are prioritised and the weak attractor for walking in step diminishes with the reduction of walking speed. Interestingly, it can be seen in Fig. 2(c) that a few subjects fixed their gaze towards the preceding walker, such as if they were concerned not to step on their foot.

The synchronisation strength index for each topological connection for normal and slow walking is shown it the fourth column in Table 3. Comparison with data in Figs. 9 and 10 shows that the values in are often in excess of an order of magnitude lower. This is because these values were obtained from a cumulative phase difference distribution for a given topological connection as has been explained in the first paragraph of Section 3.1.4. The significance of this result is that that any phase matching between a pair of subjects is relatively random, as observed in [9]. However, it can expected that the densification of a crowd can lead to the emergence of persistent phase difference patterns for front-to-back pedestrian arrangements. This is evident from the results for $C_{0,1}$ as shown in Fig. 12(b), where the positive phase difference values occur almost twice as often as the negative phase difference values.

3.2. Pedestrian-structure interaction

Pedestrian-structure interaction was quantified using the methodology introduced in Section 2.5, based on time-aligned data of a single point vertical acceleration response of BB and vertical pedestrian acceleration measured at L5.

The considered mode of vibration has a few nodes, i.e. points on the structure for which the amplitude of vibration at that mode is equal zero [41] (see Fig. 1). This causes the phase of bridge motion in that mode to be non-uniform across the structure. Since the considered mode is real rather than complex, meaning it can be represented as a stationary wave, the relative phase difference between each pair of points on the adjacent parts of the structure separated by a single node is exactly π. To account for this effect and construct a suitable signal from the bridge for analysis of HSI, information on instantaneous pedestrian location is required. This is unlike for analyses of HSI for activities in which the occupant of the structure remains stationary, for example as for jumping and bouncing on grandstands [42]. Every time the pedestrian passes the location of a node there is an abrupt change in the direction of structural response vector which can be accounted for by changing the sign of the measured bridge acceleration (i.e. at the measurement point – see Fig. 1). The knowledge of instantaneous pedestrian location relative to the mode shape also allows the response amplitude of the bridge at that location to be determined based on a single point measurement of bridge response. This is achieved by scaling the measured vibration amplitude according to the ratio of the modal amplitudes at the locations of the measurement point and the pedestrian. Since the method of analysis presented in Section 2.5 relies on phase difference only (see Eq. (6)), this step in data processing is not essential, but it allows the influence of vibration amplitude of pedestrian-structure interaction to be assessed.

The initial and end location of each pedestrian during each test hence the distance travelled, and the durations of tests were known (see Section 2.4). To determine the timing when each pedestrian passes the location of a node an assumption of constant walking speed was adopted. This might introduce an offset in phase difference due to misidentification of instances of node crossing [18] therefore the results of the assessment of directionality of HSI should be made with care. However, since the position of each pedestrian relative to others was fairly constant during each test due to the imposed requirement of preserving group cohesion, it can be expected that the phase difference between the bridge and pedestrian motion between all subjects should be affected by the constant speed assumption in a similar manner. Bearing this in mind, the mean HHI and HSI synchronisation strength indices over all instances of a given interaction (15 for HHI, i.e. for each pair of pedestrians, and 6 for HSI, i.e. for each pedestrian and the structure) were calculated, denoted hereafter as γ_{HHI}^{5s} and γ_{HSI}^{5s}, respectively. A centred moving average was used for these indices to be aligned with the bridge response data. A window extending two and a half seconds towards past and future events was chosen, containing approximately ten bridge vibration cycles in the considered mode, to provide sufficient amount of data for use in Eq. (7). The moving window was decreasingly and increasingly asymmetric as the base point moves further away from the beginning and closer to the end of the record, respectively. Therefore the windows for the first and last datum were one-sided, extending towards future and past events only, respectively.

3.2.1. Simulations

To test the applicability of an assumption that the product of vertical acceleration signal from L5 and pedestrian mass can serve as a proxy for pedestrian vertical GRF in walking (see Section 2.3), the response of BB under thereby reconstructed pedestrians' force was investigated. A modal model of BB was built based on data in Fig. 1 and Section 2.1, to which moving and modal amplitude-modulated force was applied:

$$\ddot{X}(t) + 2\zeta_n \omega_n \dot{X}(t) + \omega_n^2 X(t) = \frac{1}{M_n} \sum_{i=1}^{N} F_i(t, x_i)\phi_{i,n}(x_i) \tag{11}$$

where X is the modal displacement, ζ_n is the damping ratio, ω_n is the natural frequency, M_n is the modal mass, F_i is the force amplitude of the $i-$ th pedestrian, N is the total number of pedestrians on the bridge, $\phi_{i,n}$ is the amplitude of the $n-$ th mode shape at $i-$ th pedestrian location, x_i is the $i-$ th pedestrian location, and dots over symbols represent differentiation with respect to time t. As in the case of quantifying HSI, it was assumed in simulations that pedestrians travel across the structure at a constant speed.

3.2.2. Analysis of the results

Three examples of results from tests during which pedestrians were walking from the North to the South end of BB are presented in Fig. 13. The walking formations for these tests were: $G_{3\times2}$ for data in (a) and (b), $G_{2\times3}$ for data in (c) and (d) and $G_{1\times6}$ for data in (e) and (f). The first in the set of two plots pertaining to each test presents unfiltered acceleration response data collected at the measurement point (see Fig. 1), the same data but filtered with two-way fourth-order Butterworth band-pass filter with cut-off frequencies $f_n \pm 0.05$ Hz, 5 s root-mean-square (RMS) curve associated with the measured and filtered data, and the corresponding 5 s RMS curve obtained from simulations as explained in Section 3.2.1. The second plot presents the average 5 s synchronisation index (see Eq. (10)) for HHI and HSI, i.e. γ_{HHI}^{5s} and γ_{HSI}^{5s}, respectively. To facilitate reading the results, the magnitude of BB acceleration response at the average group location is also denoted on that plot by a grey patch. To avoid the effects of initial and end conditions associated with the experimental protocol, the data from the first and last five seconds of the test, corresponding to the gait initiation and termination stages, will not be considered
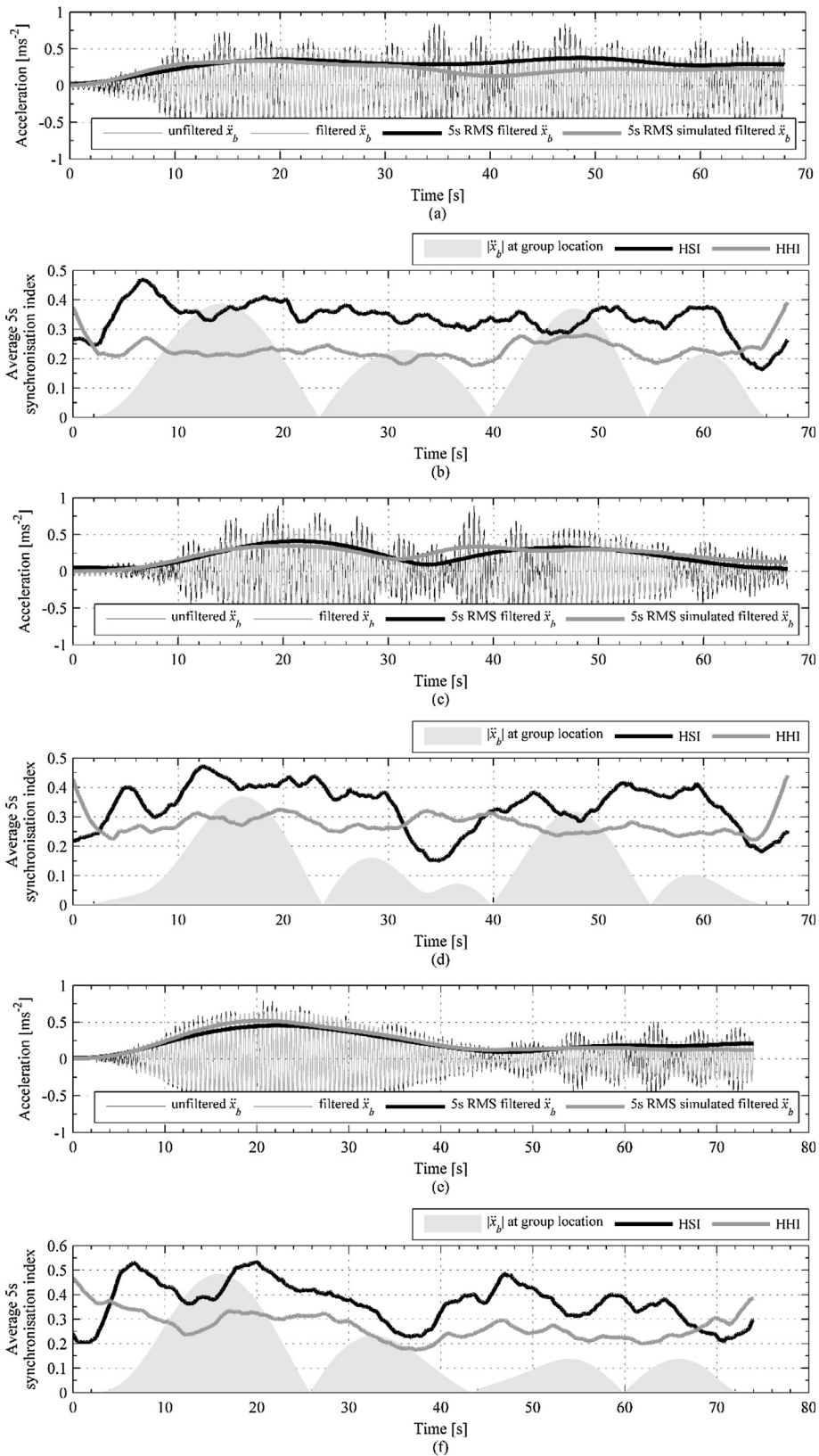
Fig. 13. Results from three tests with six pedestrians crossing BB, walking in: $G_{3\times2}$ (a) & (b), $G_{2\times3}$ (c) & (d) and $G_{1\times6}$ (e) & (f).

in the following statistical assessment of the results. The effects of initial and end conditions manifest themselves in the consistently high values of γ_{HHI}^{5s} at the beginnings and ends of the tests from which the data are presented in Fig. 13.

It can be seen in Fig. 13(a), (c) and (e) that the response of BB at the measurement point is indeed dominated by the motion in the considered mode, and that the measured and simulated BB responses at that mode are generally closely matched. The maximum magnitude of the acceleration response reached 0.53, 0.59 and 0.65 ms^{-2} for $G_{3\times2}$, $G_{2\times3}$ and $G_{1\times6}$, respectively. For comparison, the maximum BB acceleration response under the action of a single pedestrian of the mass and height close to the average values of the group, walking from the North to the South end of the bridge with a pacing rate set to excite the considered mode (2 Hz) was 0.15 ms^{-2} [18]. Clearly, the BB response due to a passage of multiple pedestrians does not, in this case, scale linearly with the response of a 'tuned' walker. However, an increase in structural response is evident with the number of pedestrian pairs walking front-to-back, which seems to agree with the affinity of this factor to HHI strength discussed in Section 3.1.2.

The RMS errors in the simulated 5 s acceleration response are 0.094, 0.064 and 0.041 ms^{-2} for $G_{3\times2}$, $G_{2\times3}$ and $G_{1\times6}$, respectively, corresponding to absolute errors in the maximum 5 s RMS BB acceleration response of 0.041, 0.067 and 0.065 ms^{-2}. This is considered a reasonable result, although it needs to be borne in mind that the pedestrian force reconstruction was based on data from L5 rather than the seventh cervical vertebra (located at the back of the neck), which was shown to be more suitable for this purpose [18]. Furthermore, some discrepancy between the results can be associated by the adopted assumption of constant speed of the walkers.

The magnitude of γ_{HSI}^{5s} is generally larger than that of γ_{HHI}^{5s}, except at the beginnings and ends of the records, and between 32 and 39 s for $G_{2\times3}$ (see Fig. 13(d)). This might indicate that it is HSI rather than HHI which was a prevalent mechanism contributing to the response of BB during the considered tests. However, the nature of this interaction needs more consideration. A recent review paper on the subject [4] noted that, while most of the empirical evidence supports the notion that the presence of walking pedestrians results in additional damping to the vertical structural modes, some modelling observations suggest that, in some specific circumstances, this condition might be reversible. This is due to the effect of the structural motion modifying the timing of pedestrian footsteps [43], and indeed the latest results from pedestrians walking on laterally oscillating treadmill give some supporting empirical evidence to this [44,45]. A similar experimental setup to the one used in [44,45], but based on a vertically-driven instrumented treadmill, was recently used to study synchronisation of walkers to ground motion in Nessler et al. [46]. It was found based on kinematics that pedestrians can intermittently lock their phase to vertical ground motion, that the modification of the timing of their footsteps depends on the relationship between the treadmill vertical oscillation and step frequencies, that synchronisation is more likely to occur for higher vibration amplitudes, and that the tendency of a pedestrian to synchronise their gait to vertical ground motion is generally stronger than that of a pair of pedestrians to synchronise their gait during side-by-side walking. This is in line with the predictions of a model [43] and the results of this study.

The existence of pedestrian-induced self-excited (i.e. motion dependent) forces identified in [43] was confirmed in the study of Dang and Živanović [2]. Their experimental protocol involved a pedestrian walking on a treadmill mounted at the centre of simply supported slab, mechanically excited at the frequency of 2 Hz, matching the frequency of the considered mode of the BB, to the acceleration amplitude comparable to those observed on the BB. An inverse force reconstruction procedure was applied to pedestrian kinematic data obtained with an optical motion capture system. It was estimated that the equivalent added damping and mass due to the presence of a pedestrian was in the range of 2.5–5 kN s m^{-1} and -100 to 700 kg, respectively. A preceding study by Georgakis and Jørgensen [47] with multiple pedestrian occupancy on a simply supported steel footbridge gave comparable equivalent added damping and the equivalent added mass equal to 102% of the pedestrian's mass. Those results were obtained based on the measured response of the bridge, considering the energy dissipated during each vibration cycle of the structure. Neither of these studies, however, presented data allowing step-to-step variations in the exchange of the energy between the pedestrian and structure to be evaluated. Further studies, enabling the direct identification of self-excited pedestrian forces on vertically oscillating structures, could greatly help in the interpretation of the results presented herein. For example, the outline of the grey patch in Fig. 13(d), representing the magnitude of BB acceleration response at the average group location, decreases locally when γ_{HSI}^{5s} is at its minimum of 0.15 at around 34 s, while γ_{HHI}^{5s} remains then relatively high at 0.3. In contrast, in Fig. 13(f) both γ_{HSI}^{5s} and γ_{HHI}^{5s} have local minima at 0.23 and 0.18, respectively, at the same spatial group location relative to the mode shape, i.e. the second modal segment counting from the North end of BB, between the second and third nodes crossed at 26 and 44 s, respectively. No considerable decrease in BB acceleration response at the group's location is therein visible. The reason for this difference is currently unknown.

Relatively little variability can be seen in γ_{HHI}^{5s}, for which the coefficients of variation are 11.23, 8.84 and 17.2% for $G_{3\times2}$, $G_{2\times3}$ and $G_{1\times6}$, respectively. In comparison, the coefficients of variation for γ_{HSI}^{5s} are 10.51%, 20.25% and 19.45%, respectively. This might be caused by an adaptive pedestrian behaviour in response to bridge motion manifesting itself by intermittent changes to the timing of footsteps. This is in line with recent findings of Dang and Živanović [2].

4. Conclusions

This paper reports results from a series of tests with six pedestrians crossing a footbridge. A wireless sensor network of motion monitors was used to obtain data on pedestrians' vertical force, time-synchronised with vertical bridge response data

obtained with a set of wired accelerometers. This allowed pedestrian-pedestrian and pedestrian-structure interaction to be investigated.

A bivariate analysis framework was proposed and applied to study pedestrian-pedestrian and pedestrian-structure interactions encompassing wavelet transform, synchronisation measures derived from Shannon entropy and circular statistics.

A topological pedestrian interaction map was contrived showing the strength of synchronisation between pedestrians. The strongest correlation in pedestrians' gait occurred for a pair walking front-to-back, followed by a pair walking side-by-side, but the correlation was found to weaken the further the distance of the synchronisation stimulus from the observer. The strength of synchronisation assigned to the topological pedestrian map shows right side bias relative to the observer, which might be a behavioural effect caused by ocular dominance. A negative correlation between the magnitude of pairwise pedestrian height difference and synchronisation strength was observed, in line with the results previously reported by others limited to side-by-side walking. Considering the extent of the conducted tests, this may indicate a synchronised state is indeed a relatively weak attractrix of the system consisting of two walking pedestrians when visual motion cues from a fellow pedestrian are available.

The influence of walking formation on synchronisation strength was examined, revealing that the more linkages in the walking formation in which pedestrians are faced front-to-back the stronger the average synchronisation index. This indicates that synchronisation can be promoted by the self-organisation mechanism taking place in crowds of walkers, manifesting itself in formation of lanes, e.g. moving in opposite directions.

The analysis of synchronisation directionality showed that for a pair of pedestrians walking front-to-back there is a weak tendency for the follower to initiate steps at the same time or faster than the leader. Slower walking speed causes this effect to be stronger. This might be associated with anticipatory strategy in adaptive stepping behaviour, whereby the follower will try to reach the double-support phase of gait slightly faster than the leader. This is because in this phase of gait the stance is more stable and corrections to the body motion can be implemented more easily in order to avoid collision with the leader or to preserve grid cohesion. For a pair of pedestrians walking side-by-side, there is a weak tendency to walk in step, bearing in mind no distinction is made in this study between steps initiated with ipsilateral and contralateral leg since this is irrelevant from the point of view of structural stability in the considered (vertical) vibration mode.

The analysis of pedestrian-structure interaction revealed a stronger tendency of pedestrians to coordinate their behaviour and force with the structural motion rather than with each other. This supports efforts of the scientific community spent on gaining knowledge of the fundamental relations governing pedestrian behaviour while walking on moving structures. However, to further our understanding of the coupled crowd-structure system dynamics, the effect of between-subjects interaction also needs to be considered. A methodology addressing this issue was proposed in this study. Therefore this study contributes to the development of a new class of pedestrian loading models, calibrated based on data representative of real pedestrian behaviour on full-scale structures.

Acknowledgements

References

[1] D. Helbing, P. Molnar, Social force model for pedestrian dynamics, Phys. Rev. E 51 (1995) 4282–4286.
[2] H.V. Dang, S. Živanovic, Influence of low-frequency vertical vibration on walking locomotion, J. Struct. Eng. 142 (12) (2016) 04016120 (1–12).
[3] C.C. Caprani, E. Ahmadi, Formulation of human-structure interaction system models for vertical vibration, J. Sound Vib. 377 (2016) 346–367.
[4] E. Shahabpoor, A. Pavic, V. Racic, Interatcion between walking humans and structures in vertical direction: a literature review, Shock Vib. 3430285 (2016) 1–22.
[5] H. Bachmann, W. Ammann, Vibrations in Structures Induced by Man and Machines, IABSE, Zurich, Switzerland, 1987.
[6] H. Grundmann, H. Kreuzinger, M. Schneider, Schwingungsuntersuchungen für Fußgängerbrücken (Vibration tests of pedestrian bridges in German), Der Bauingenieur 68 (1993) 215–225.
[7] C. Butz, M. Feldmann, C. Heinemeyer, G. Sedlacek, B. Chabrolin, A. Lamaire, M. Lukić, P.-O. Martin, E. Caetano, Á. Cunha, A. Goldack, A. Keil, M. Schlaich, Advanced Load Models for Synchronous Pedestrian Excitation and Optimised Design Guidelines for Steel Footbridges, European Commission, Brussels, Belgium, EUR 23318 EN, 2008.
[8] M.C. Araújo Jr, H.M.B.F. Brito, R.L. Pimentel, Experimental evaluation of synchronisation in footbridges due to crowd loading, Struct. Eng. Int. 19 (2009) 298–303.
[9] F. Ricciardelli, A. Pansera, An experimental investigation into the interaction among walkers in groups and crowds, in: 10th International Conference on Recent Advances in Structural Dynamics, 12–14 July 2010, Southampton, UK.
[10] K. Van Nimmen, G. Lombaert, I. Jonkers, G. De Roeck, P. Van den Broeck, Characterisation of walking loads by 3D inertial motion tracking, J. Sound Vib. 333 (2016) 5212–5226.
[11] Q. Li, J. Fan, J. Nie, Q. Li, Y. Chen, Crowd-induced random vibration of footbridge and vibration control using multiple tuned mass dampers, J. Sound Vib. 329 (2010) 4068–4092.
[12] A.Z. Zivotofsky, J.M. Hausdorff, The sensory feedback mechanisms enabling couples to walk synchronously: an initial investigation, J. Neuroeng. Rehabil. 4 (28) (2007) 1–5.
[13] N.R. van Ulzen, C.J.C. Lamoth, A. Daffertshofer, G.R. Semin, P.J. Beek, Stability and variability of acoustically specified coordination patterns while walking side-by-side on a treadmill: does the seagull effect hold?, Neurosci Lett. 474 (2) (2010) 79–83.
[14] A.Z. Zivotofsky, L. Gruendlinger, J.M. Hausdorff, Modality-specific communication enabling gait synchronization during over-ground side-by-side walking, Hum. Move. Sci. 31 (2012) 1268–1285.

[15] J.A. Nessler, S.J. Gilliland, Interpersonal synchronization during side by side treadmill walking is influenced by leg length differential and altered sensory feedback, Hum. Move. Sci. 28 (2009) 772–785.
[16] M. Moussaid, N. Perozo, S. Garnier, D. Helbing, G. Theraulaz, The walking behaviour of pedestrian social groups and its impact on crowd dynamics, PLoS ONE 5 (4) (2010) e10047.
[17] J.M.W. Brownjohn, P. Reynolds, S.K. Au, D. Hester, M. Bocian, Experimental modal analysis of civil structures: state of the art, in: SHMII – 7th International Conference on Structiural Health monitoring of Intelligent Infrastructure, 1–3 July 2015, Turin, Italy.
[18] M. Bocian, J.M.W. Brownjohn, V. Racic, D. Hester, A. Quattrone, R. Monnickendam, A framework for experimental determination of localised vertical pedestrian forces on full-scale structures using wireless attitude and heading reference systems, J. Sound Vib. 367 (2016) 217–243.
[19] J.M.W. Brownjohn, M. Bocian, D. Hester, A. Quattrone, W. Hudson, D. Moore, S. Goh, M.S. Lim, Footbridge system identification using wireless inertial measurements units for force and response measurements, J. Sound Vib. 384 (2016) 339–355.
[20] P.S. Addison, The Illustrated Wavelet Transform Handbook: Introductory Theory and Applications in Science, Engineering, Medicine and Finance, first ed., Institute of Physics Publishing, Bristol, UK, 2002.
[21] M. Rosenblum, A. Pikovsky, J. Kurths, C. Schäfer, P.A. Tass, Phase synchronization: from theory to data analysis, Handb. Biol. Phys. 4 (2001) 279–321.
[22] P.A. Tass, M.G. Rosenblum, J. Weule, J. Kurths, A. Pikovsky, J. Volkmann, A. Schnitzler, H.-J. Freund, Detection of n:m phase locking from noisy data: application to magnetoencephalography, Phys. Rev. Lett. 81 (1998) 3291–3294.
[23] J. Bodgi, S. Erlicher, P. Argoul, O. Flamand, F. Danbon, Crowd-structure synchronisation: coupling between Eulerian flow modeling and Kuramoto phase equation, in: Footbridge – 3rd International Conference, 2–4 July 2008, Porto, Portugal.
[24] F. Durupınar, U. Güdükbay, Visualization of crowd synchronization on footbridges, J. Visual. Japan 13 (2010) 69–77.
[25] B. Eckhardt, E. Ott, S.H. Strogatz, D.M. Abrams, A. McRobie, Modeling walker synchronization on the millennium bridge, Phys. Rev. E 75 (2007) 1–10.
[26] T. Morbiato, R. Vitaliani, A. Saetta, Numerical analysis of a synchronization phenomenon: pedestrian–structure interaction, Comput. Struct. 89 (2011) 1649–1663.
[27] F. Venuti, L. Bruno, N. Bellomo, Crowd dynamics on a moving platform: mathematical modelling and application to lively footbridges, Math. Comput. Model. 45 (2007) 252–269.
[28] W.H. Howell, Medical Physiology and Biophysics, Sounders, London, UK, 1960.
[29] C. Porac, S. Coren, The dominant eye, Psychol. Bull. 83 (1976) 880–897.
[30] A.P. Mapp, H. Ono, R. Barbeito, What does the dominant eye dominate? A brief and somehow contentious review, Percept. Psychophys. 65 (2003) 310–317.
[31] E. Shneor, S. Hochstein, Eye dominance effects in feature search, Vision Res. 46 (2006) 4258–4269.
[32] E. Shneor, S. Hochstein, Eye dominance effects in conjunction search, Vis. Res. 48 (2008) 1592–1602.
[33] K. Hutcheson, A test comparing diversities based on the Shannon formula, J. Theor. Biol. 29 (1970) 151–154.
[34] D. Helbing, A. Johansson, Pedestrian, crowd and evacuation dynamics, Encycl. Complex. Syst. Sci. 16 (2010) 6476–6495.
[35] G.A. Dean, An analysis of the energy expenditure in level and grade walking, Ergonomics 8 (1965) 31–47.
[36] J.A. Nessler, G. Kephart, J. Cowell, C.J. De Leone, Varying treadmill speed and inclination affects spontaneous synchronisation when two individuals walk side by side, J. Appl. Biomech. 27 (2011) 322–329.
[37] R.M. Alexander, Principles of Animal Locomotion, Princeton University Press, Princeton, USA, 2003.
[38] R.M. Alexander, Optimization and gaits in the locomotion of vertebrates, Physiol. Rev. 69 (1989) 1199–1227.
[39] J.E.A. Bertram, A. Ruina, Multiple walking speed-frequency relations are predicted by constrained optimization, J. Theor. Biol. 209 (2001) 445–453.
[40] P. Berens, CircStat: a MATLAB toolbox for circular statistics, J. Stat. Softw. 31 (10) (2009).
[41] D.J. Ewins, Modal Testing: Theory, Practice and Application, second ed., Research Studies Press Ltd., Baldock, England, 2001.
[42] A. Quattrone, M. Bocian, V. Racic, J.M.W. Brownjohn, E.J. Hudson, D. Hester, J. Davies, Characterisation of transient actions onduced by spectators on sport stadia, in: Proceedings of the 34th IMAC – A Conference and Exposition on Structural Dynamics, Orlando, USA, 25–28 January 2016.
[43] M. Bocian, J.H.G. Macdonald, J.F. Burn, Biomechanically inspired modeling of pedestrian-induced vertical self-excited forces, J. Bridge Eng. 18 (12) (2013) 1336–1346.
[44] M. Bocian, J.H.G. Macdonald, J.F. Burn, D. Redmill, Experimental identification of the behaviour of and lateral forces from freely-walking pedestrians on laterally oscillating structures in a virtual reality environment, Eng. Struct. 105 (2015) 62–76.
[45] M. Bocian, J.F. Burn, J.H.G. Macdonald, J.M.W. Brownjohn, From phase drift to synchronisation - pedestrian stepping behaviour on laterally oscillating structures and consequences for dynamic stability, J. Sound Vib. 392 (2017) 382–399.
[46] J.A. Nessler, S. Heredia, J. Bélair, J. Milton, Walking on vertically oscillating treadmill: phase synchronization and gait kinematics, PLoS ONE 12 (1) (2017) e0169924.
[47] C.T. Georgakis, N.G. Jørgensen, Change is mass and damping on vertically vibrating footbridges due to pedestrians, in: Proceedings of the 31st IMAC – A Conference and Exposition on Structural Dynamics, Garden Grove, USA, 11–14 February 2013.